

# AN APPLICATION OF MICROALLOYING AND THERMOMECHANICAL ROLLING IN SBQ LONG PRODUCTS\*

Rafael Stella Galdino<sup>1</sup>  
Carolina Conter Elgert<sup>2</sup>  
Marcos Paulo da Silveira<sup>3</sup>  
Messias Prado de Almeida<sup>4</sup>  
Samuel Henrique Freese<sup>5</sup>  
José Roberto Bolota<sup>6</sup>

## Abstract

Microalloyed steels have been intensely studied as an alternative to increase strength by grain refinement and/or precipitation hardening. Long steel products have a wide range of opportunities to apply well-defined principles of controlled rolling (CR) in order to increase strength and toughness with reduced costs. To evaluate the effect of microalloying elements as Nb and Ti with thermomechanical treatment, three conditions were tested: DIN 16MnCrS5 with hot rolling (HR), DIN 16MnCrS5 with Nb and CR and DIN 16MnCrS5 with Nb+Ti and CR. Austenitic grain size, obtained by direct quenching after rolling, has shown a decrease 32% with Nb addition, and 29% when Nb and Ti was added. Controlled rolling generated higher grain refinement and pancaked grains near the surface. When comparing ferritic grain size, controlled rolling plus niobium and titanium additions resulted in significant reduction of 35%. Yield strength increased 15% with microalloying and CR and more than 270% in impact toughness, even at -40°C.

**Keywords:** Thermomechanical Rolling; Niobium; Long Products; Grain Size.

<sup>1</sup> Engineer, Specialist, RD&I, Gerdau, Pindamonhangaba, São Paulo, Brazil.

<sup>2</sup> MSc., Senior Specialist, RD&I, Gerdau, Charqueadas, Rio Grande do Sul, Brazil.

<sup>3</sup> Engineer, Technical Manager, Process Engineering, Gerdau, Pindamonhangaba, São Paulo, Brazil.

<sup>4</sup> Technician, Analyst, RD&I, Gerdau, Pindamonhangaba, São Paulo, Brazil.

<sup>5</sup> MSc., Manager, RD&I, Gerdau, Pindamonhangaba, São Paulo, Brazil.

<sup>6</sup> Engineer, Consultant, Technical Assistance, CBMM, São Paulo, São Paulo, Brazil.

## 1 INTRODUCTION

Steels in the automotive industry, in general, must achieve high strength levels without sacrificing other properties such as ductility and toughness. Among several alternatives, grain refinement is a key technique for increasing the strength and toughness of metals simultaneously [1].

The principal goal of microalloying additions is ferrite strengthening by grain refinement, precipitation hardening and solid solution strengthening. Titanium, niobium and vanadium are very effective as microalloying elements in steel, influencing the microstructure by both a solute drag effect and the formation of nitrides and carbides [2].

Recently, considerable work has been focused upon throughout the world studying the addition of Nb to long product applications assisting the steelmaker in minimizing raw materials costs in hot rolled beams, rebar and forgings [3].

For long product applications, the design of alloying and corresponding processing routine is based on the specific needs, mechanical properties, machinability, cold formability, high temperature carburizing, section size and shape of each application. [4].

In general, higher carbon content is required due to hardenability definitions. However, the solubility of Nb products decrease as carbon content increase, as demonstrated in figure 1 [3,4].

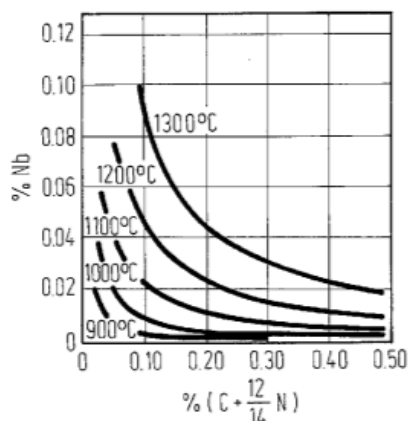


Figure 1. Nb(C,N) solubility in austenite [3].

The rolling process of bar rolling mills are different from well-known plate and hot strip mills:

- Short reheating time in temperatures that do not usually allow for complete precipitates dissolution;
- Layouts are usually continuous, which means that interpass times are shorter than plates and hot strip mills;
- Pass design are pre-defined with relatively fixed groove design, with box, diamond, oval and round shapes.
- As dimensional tolerances should be tight, low deformation in finishing passes are common and necessary.

De Ardo [5] review article points out that small deformations promote shorter times for precipitation. Because of the important influence of interpass time, solute effects would become more important, and the inhibition of recrystallization largely takes place by means of solute drag. In solid solution, microalloying elements retard all diffusion-controlled processes [2,5,6], as shown in Figure 2.

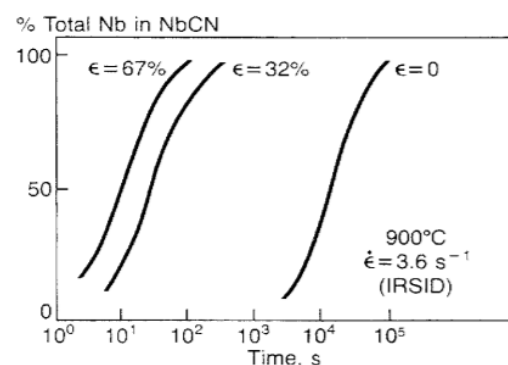


Figure 2. Influence of strain level on kinetics of NbCN precipitation at 900°C in steel containing 0.17C-0.04Nb-0.011N [5]

Niobium is the most effective of the three micro-alloying elements in this context, followed by titanium. During hot rolling of steel, the solute drag effect assists in grain refinement by preventing

secondary grain growth during the interpass time, since grain growth is a diffusion-controlled process [2,5,6].

The aim of this work is to investigate microalloying and processing contributions in long products in order to obtain high strength and high toughness steels for engineering bars (SBQ – Special Bar Quality).

## 2 MATERIAL AND METHODS

The chemical composition, rolling schedule, mechanical properties and microstructure analysis are described below. Figure 3 summarizes the methodology. Using DIN 16MnCrS5 base composition, effect of Nb and Nb+Ti were analyzed after controlled rolling and compared to standard steel with AlN as grain refiner.

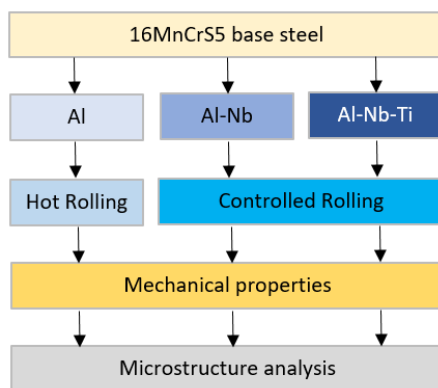


**Figure 3.** Summary of the tests performed in this article.

### 2.1 Chemical compositions

Three heats were produced in an EAF melt shop according to the compositions of a DIN 16MnCrS5 steel showed in the Table 1. As can be seen, different combinations of Al, Nb and Ti were produced.

All three heats were vacuum degassed and casted by a continuous casting machine with a 155mm square section.

**Table 1.** Chemical composition of DIN 16MnCrS5.

Steel	C	Mn	Si	P	S
Al	0,19	1,16	0,25	0,017	0,020
Al-Nb	0,19	1,13	0,24	0,017	0,025
Al-Nb-Ti	0,18	1,14	0,22	0,015	0,022
Cr	Ni	Mo	Cu	Al+Nb+Ti*	N*
1,12	0,09	0,03	0,14	200 - 400	<100
1,02	0,15	0,04	0,15	400 - 700	>100
1,04	0,16	0,04	0,15	400 - 1000	>100

\* values in ppm.

### 2.2 Rolling schedule

Critical temperatures of the steels were calculated following equations 1 to 5 in order to define the best parameters for rolling.

The solubilization temperature of niobium carbonitrides was calculated using Irvine's equation (1), considering the effect of titanium as effective nitrogen content in equation (2) [7]. According to Barbosa [8], private communication, Irvine's equation has been giving a good approach considering a valid Nb range, even with higher carbon content.

$$T \geq 6770 / (2.26 - \log([\text{Nb}][\text{C} + (12/14) * \text{N}])) \quad (1)$$

$$\text{Neff} = [\text{N}] - (14/48) [\text{Ti}] \quad (2)$$

Non-recrystallization temperature ( $T_{nr}$ ), temperatures for 95% (RLT) and 5% (RST) of recrystallization was also calculated according to equations 3, 4 and 5, and Ar3 obtained by equation 6 [2,7,9,10].

$$T_{nr} = 887 + 464\text{C} + 6445\text{Nb} - 644\text{Nb}^{0.5} + 732\text{V} - 230\text{V}^{0.5} + 890\text{Ti} + 363\text{Al} - 357\text{Si} \quad (3)$$

$$\text{RLT} = 174 \log([\text{Nb}][\text{C} + (12/14)\text{N}] + 1444) \quad (4)$$

$$\text{RST} = \text{RLT} - 75 \quad (5)$$

$$\text{Ar3} = 910 - 310\text{C} - 80\text{Mn} - 20\text{Cu} - 15\text{Cr} - 55\text{Ni} - 80\text{Mo} \quad (6)$$

Two types of rolling were defined combining with three different heats:

- Standard steel (Al) was processed by hot rolling (HR), named as “Al-HR”;
- Controlled rolling steels with Al-Nb and Al-Nb-Ti additions were named as “Al-Nb-CR” and “Al-Nb-Ti-CR”, respectively.

Al-steel was not controlled rolled because of low recrystallization temperatures required and no niobium available to promote recrystallization delay.

Figure 4 shows a schematic design of the rolling processes used in this work.

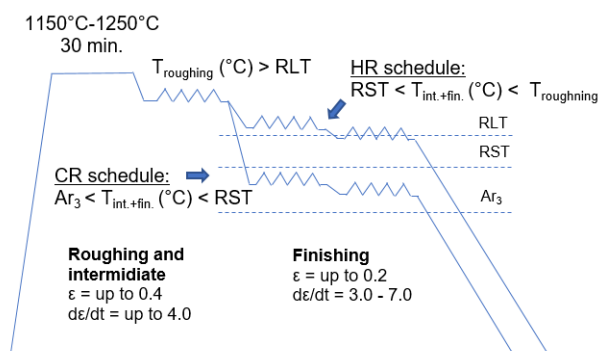


**Figure 4.** Hot rolling schedules used during rolling.

Billets of the 3 steels were reheated and soaked for 30 minutes, descaled and rolled in a continuous rolling mill, passing through roughing, intermediate passes, and a finishing passes schedule with a 3-roll technology equipment (*Kocks block*). Reductions in finishing passes are small, in order to achieve tight dimensional tolerances, as bar rolling of SBQ steels require.

Hot rolling process with the Al-steel was performed with the roughing temperature higher than RLT ( $T_{roughing}$ ) and intermediate and finishing temperatures ( $T_{int.+fin}$ ) achieved partial recrystallization region.

Controlled rolling process of Nb and Nb+Ti consisted on performing roughing passes in  $T_{roughing}$  higher than RLT and intermediate and finishing temperatures among RST and  $A_{r3}$ .

All three conditions were cooled in the same cooling rate 0,5-1,0°C/s.

Samples right after the last pass were cut for austenitic grain size evaluation.

### 2.3 Mechanical Properties and microstructure analysis

Ultimate tensile strength (UTS), Yield Strength (YS), Reduction of Area (ROA), Elongation (El.) and Charpy tested in 20°C (I 20°C) and -40°C (I -40°C) were statistically evaluated by analysis of variance (ANOVA) and compared with Games-Howell test to define which of the steels have statistically different results. The level of significance used was 5%, meaning that if *p-value* lower than 5%, a significant difference would be found.

5 samples for tensile tests and 6 samples for V-notched Charpy tests were cut for each steel, according to Figure 5.

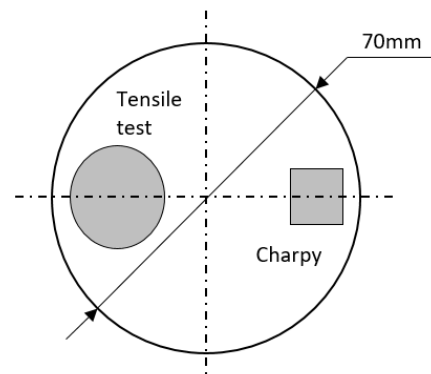


**Figure 5.** Position of sampling viewed from transverse section

Microstructure of the region among  $\frac{1}{4}$  and  $\frac{1}{2}$  radius of the longitudinal section was evaluated with Nital 2% etching and grain size was evaluated with linear intercept method according to ASTM E112.

Austenitic grain size of samples quenched after last pass during rolling were analyzed. The region among  $\frac{1}{4}$  radius and  $\frac{1}{2}$  radius of the longitudinal section was evaluated with 2% picric acid aqueous solution etching and grain size was measured with linear intercept method according to ASTM E112.

The same statistical methods were used to compare austenitic grain size and ferritic-perlitic grain size.

### 3 RESULTS AND DISCUSSION

#### 3.1 Chemical composition and rolling schedule

The critical temperatures for the rolling schedule were calculated according to equations 1-5, and are showed in table 2. Nb and Ti enables controlled rolling to be done in current rolling mill layout. As chemical compositions use the same steel base (DIN 16MnCrS5), Ar<sub>3</sub> values were the same. For this reason, unless precipitates effects, ferrite transformation should occur in similar temperatures. The temperature of the final passes was also higher than Ar<sub>3</sub>.

**Table 2.** Critical temperatures for tested alloys.

Steel	T <sub>sol</sub> Nb	T <sub>nr</sub>	RST	RLT	Ar <sub>3</sub>
Al	984	872	846	921	734
Al-Nb	1295	1033	1009	1084	731
Al-Nb-Ti	1296	1067	1012	1087	733

Controlled rolling generated pancaked grains in the surface, but with a mixing of fine equiaxed, big elongated and fine elongated grains (figure 6). As a temperature prediction is not feasible yet, a hypothesis should be considered: temperature variation in the cross section of the bar, leading to partial recrystallization. Authors advice that high reduction rates in temperatures below T<sub>nr</sub> are necessary to take advantage of controlled rolling [1][6].

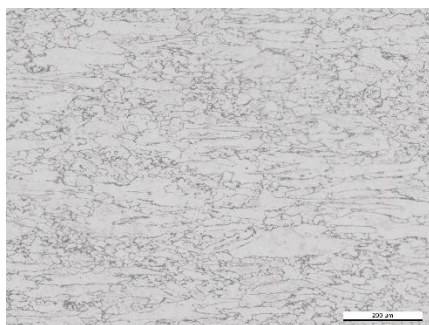


**Figure 6.** Austenitic grain size of surface longitudinal section of Al-Nb controlled rolled.

Etched with aqueous solution of picric acid.  
Magnification 100x;

Even though, figure 7 shows grain refinement in figures (b) and (c), which represents mid radius of longitudinal sections, compared to Al-HR steel (a). Table 3 shows mean austenitic grain size for mid radius regions of the three steels.



(a)



(b)



(c)

**Figure 7.** Austenitic grain size of mid-radius longitudinal section of (a) Al-HR, (b) Al-Nb-CR and (c) Al-Nb-Ti-CR. Etched with aqueous solution of picric acid 2%. 100x magnification.

**Table 3.** Austenitic (A) grain size measurements

Steel	A (μm)
Al-HR	30,3±2,8
Al-Nb CR	20,6±1,4
Al-Nb-Ti CR	21,5±1,4

Nb and Nb-Ti added steels have shown an important grain refinement

compared to Al-HR. However, no difference in grain size could be found among Al-Nb-CR and Al-Nb-Ti-CR steels.

It is possible that the main cause for grain refinement in obtained were solute drag mainly by Nb addition. The interpass time and total rolling time in bar rolling mills are very short and precipitation during rolling shouldn't be extensive. The inhibition of recrystallization largely takes place by solute drag.

### 3.2 Mechanical properties

Tensile tests presented in Table 4 show a 15% increase in yield strength considering Nb-CR condition compared to standard condition (Al-HR).

Table 5 show regression coefficients and p-value for tensile tests. UTS, YS, YS/UTS, impact testing for 20°C and -40°C have shown good regression coefficients and significant difference among each steel. ROA and El. had poor correlation coefficients.

**Table 4.** Mechanical properties from tensile tests.

Properties	Al-HR	Al+Nb-CR	Al+Nb+Ti-CR
UTS (MPa)	650 ±21	616 ±4	595 ±8
YS (MPa)	380 ±18	436 ±7	403 ±7
YS/UTS (%)	58,1 ±1,5	70,8 ±1,4	67,8 ±1,8
ROA (%)	67,3 ±2,7	71,8 ±1,2	70,4 ±3,3
El. (%)	23,3 ±1,2	25,7 ±1,1	26 ±2,4
I 20°C (J)	47 ±9	174 ±5	202 ±29
I -40°C (J)	12 ±2	130 ±19	183 ±17

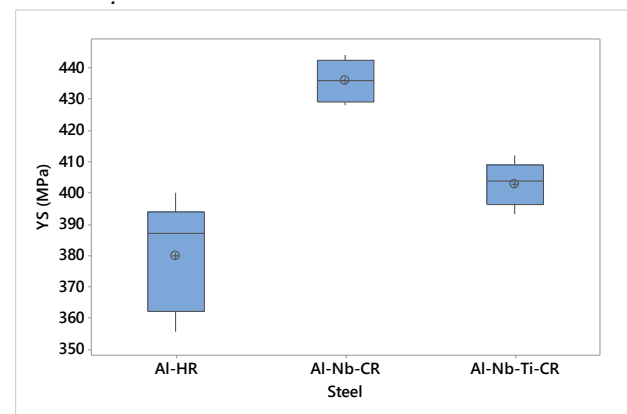
**Table 5.** Regression coefficient and p-value of ANOVA analysis of tensile tests.

Properties	P-value	R <sup>2</sup> <sub>ajust</sub> (%)
UTS	<u>0,000</u>	<u>80,31</u>
YS	<u>0,002</u>	<u>75,86</u>
YS/UTS	<u>0,000</u>	<u>92,26</u>
ROA	0,039	30,23
El.	0,033	28,98
I 20°C (J)	<u>0,000</u>	<u>92,08</u>

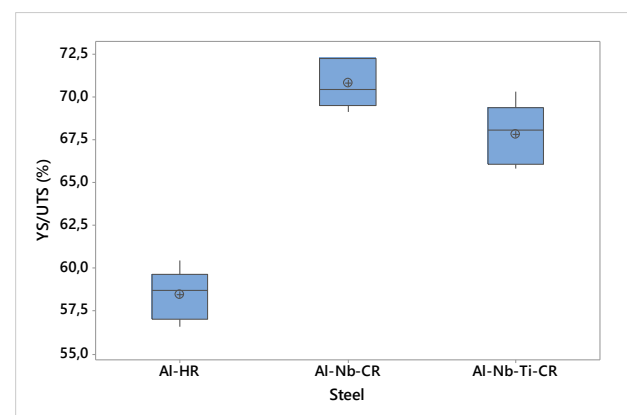
I -40°C (J)    0,000    95,03

Table 4 demonstrates that UTS values of Nb microalloyed steel were lower than Al-HR steel. However, figure 8 illustrate that Nb an Nb+Ti additions increased YS. Yet, Al-Nb-CR had a higher yield strength than Al-Nb-Ti-CR. There isn't, for YS, any statistical difference among microalloyed steels.

When correlating YS and UTS, an interesting fact should be outlined: microalloying addition increased YS/UTS (figure 9). This issue would be attributed to grain refinement and/or precipitation hardening. Nevertheless, Ti addition hasn't demonstrated influence in YS/UTS rate.



**Figure 8.** Yield strength (YS) of the steels.



**Figure 9.** Yield strength/tensile strength ratio (YS/UTS) of the steels.

Grozier and Bucher [11] proposed equations to predict yield strength (YS) and tensile strength (TS) of ferritic-pearlitic C-Mn steels in their work (equations 7 and 8). Mn and Si are the alloy content in %, "d" is the grain size in mm. Pearlite fraction "Pearl" can be calculated according to

equation 9, including C as carbon content in %.

$$YS = 95.84 + 40.68Mn + 70.4Si + 1.517Pearl + 3.282/d^{0.5} \quad (7)$$

$$TS = 223.11 + 56.74Mn + 101.97Si + 4.323Pearl + 2.344/d^{0.5} \quad (8)$$

$$Pearl = 10.7 + 110.9C + 11.3Mn + 48.4 Si \quad (9)$$

Although Cr content is not considered, a comparison with the results of this paper is reasonable. Mn, Si and carbon content of all steel are similar, grain size and pearlite fraction should explain differences in mechanical properties, regarding same cooling rate. Pearlite fraction would have higher contribution in tensile strength than in yield strength, and grain size should have higher contribution in YS.

Pickering [12] also developed an equation (9) for consider precipitated fraction ( $\Delta_{ppt}$ ), grain size ( $d_0$ ) and soluble nitrogen ( $N_{sol}$ ) on YS. Equation 10 comparably agrees with higher yield strength for microalloyed steels, adding more possible contributions.

$$YS = 88 + 37Mn + 83Si + 2918N_{sol} + 15.1/d^{0.5} + \Delta_{ppt} \quad (10)$$

For Charpy impact testing, figure 10 compares the steel in different testing temperatures. It's possible to assume that ductile-brittle transition temperature was severely reduced by microalloying addition and controlled processing.

Al-Nb-Cr and Al-Nb-Ti-CR steels presented similar behavior in room temperature, despite of higher scatter of absorbed energy results for Ti-added steel. Both of them obtained an increase of more than 350% of absorbed energy compared to the standard steel (Al-HR).

In negative temperature, Al-Nb-Ti-CR absorbed energy were higher than Al-Nb-CR. Al-HR was only 12J.

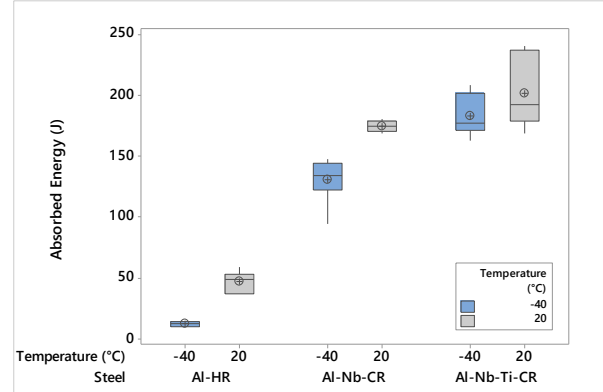


**Figure 10.** Charpy impact testing of the steels. Grey boxes represent tests in room temperature (20°C). Blue boxes are results obtained in -40°C.

In 1994, Mintz [13] defined equation 11 for impact transition temperature for C-Mn steels. Evaluating this equation is possible to see factors considered for impact transition temperature prediction: grain size in  $\mu\text{m}$  ( $d$ ), pearlite fraction ( $p$ ), cooling rate (CR), and Mn, Si, P, S contents.

$$ITT (54J) = 84.8 - 5.65/d^{0.5} + 1.76p - 53.1Si + 1490S - 1379P - 4.97CR^{0.5} - 70.1Mn \quad (11)$$

As Mn, Si, S and P content are almost the same in each steel, grain size and pearlite fraction again would play an important role in absorbed energy in low temperatures.

Table 6 summarizes differences of properties obtained by microalloying and processing. As analysis of variance proves that there is a statistical difference between conditions tested, a Games Howell comparison highlights which of the conditions are effectively different.

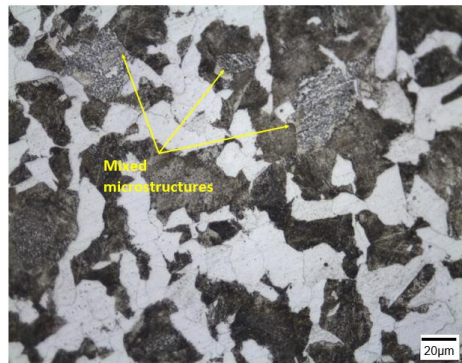
**Table 6.** Games Howell comparison among mechanical properties of the steels.

Properties	Al-Nb-CR vs. Al-HR	Al-Nb-Ti-CR vs. Al-HR	Al-Nb-Ti-CR vs. Al-Nb CR
UTS	X		
YS	X		
YS/UTS	X	X	
I 20°C (J)	X	X	
I -40°C (J)	X	X	X

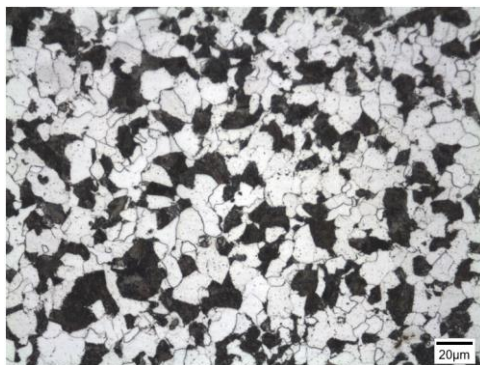
Comparisons containing "X" are statistically different.

### 3.2 Microstructure analysis

Microstructures of analyzed steels are presented in figure 11. Al-HR in (a) has higher pearlite fraction, grain size, and also some acicular microstructures inside pearlite colonies, highlighted by yellow arrows in figure 11 (a). Al-Nb-CR (b) and Al-Nb-Ti-CR (c) grain sizes were thinner and more ferrite can be seen.



(a)



(b)



(c)

**Figure 11.** Microstructures of transversal section from charpy samples tested in -40°C. (a) Al-HR, (b) Al-Nb-CR, (c) Al-Nb-Ti-CR. Nital 2% etched. Magnification 500x.

Ferritic-pearlitic grain size, in Table 7, measured by linear intercept, shows that there isn't any difference between Al-Nb-CR and Al-Nb-Ti-CR. Grain size of microalloyed steels are 34% thinner than Al-HR steel, probably due to solute drag effect in grain refinement. The grain size evaluation was performed in mid-radius region, where samples for tensile tests and charpy were taken.

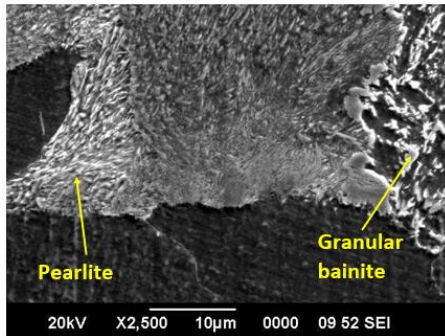
**Table 7.** Ferritic-pearlitic (F-P) grain size measurements

Steel	F-P (µm)
Al-HR	23,3±1,3
Al-Nb CR	15,3±1,1
Al-Nb-Ti CR	15,0±0,6

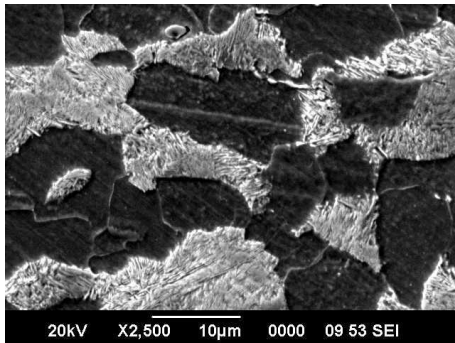
Higher pearlite colonies and lower ferrite fraction should be related to poor impact results in room temperature and -40°C.

Mixed microstructures found inside pearlite colonies are mainly granular bainite, probably associated to microinclusions. Figure 12 (a) shows pearlite and granular bainite in Al-HR steel. Figure 12 (b) presents Al-Nb-CR steel thinner pearlite colonies, apparently with lower interlamellar distance. Although all steels were air cooled, controlled rolled steels would reach cooling bed with lower temperature, leading to lower interlamellar space in pearlite.

Another interesting finding in this work was the banded microstructure in microalloyed steels. Figure 13 brings micrographs of the steels in rolling direction. The notch of charpy samples were perpendicular to the banding direction. Longitudinal section of Al-Nb-CR and Al-Nb-Ti-CR steels were severely banded, as can be seen in figure 13. Al-HR wasn't banded in the same degree.



(a)



(b)

**Figure 12.** SEM micrographs of transversal section of (a) Al-HR and (b) Al-Nb-CR. Nital 2% etched. Magnification 2500x.

Several authors [14, 15, 16] analyzed causes of ferrite-pearlite banding in steels. Banding mainly depends on three factors: the micro-segregation of alloying elements, the cooling rate during the transformation, and the austenite grain size.

During solidification, alloying elements having partition coefficients higher than 1 (ex. Mn, Si, Cr, p, S, Nb and Ti) are rejected, resulting in high solute content region. The distribution of solute provides basis for microchemical banding [16].

During cooling, the ferrite starts to nucleate in the regions with a high A3 transition temperature, which causes the carbon to redistribute. The carbon is piled up in regions with a low A3 transition temperature. The increase in carbon content will lower the local A3 transition temperature even further. Eventually, the composition in these regions becomes eutectoidic and pearlite can form if the

temperature is below the A1 transition temperature [14].



(a)



(b)

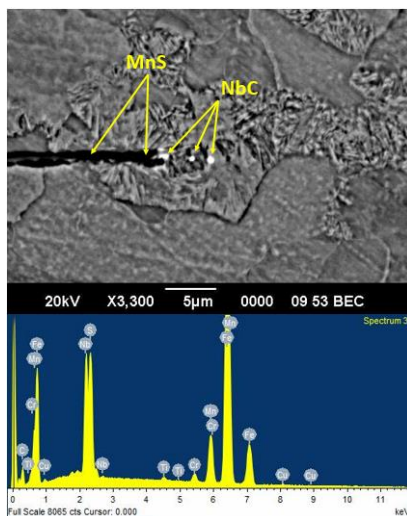


(c)

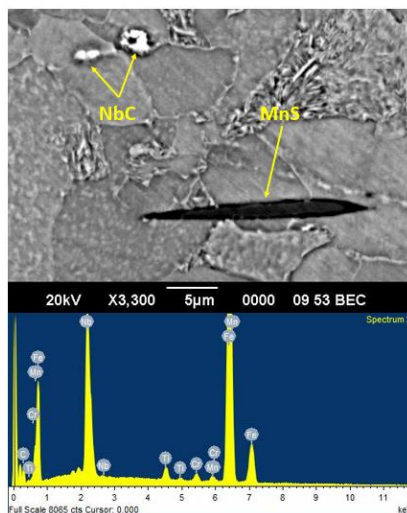
**Figure 13.** Microstructures of mid-radius longitudinal section of (a) Al- HR, (b) Al-Nb-CR e (c) Al-Nb-Ti-CR. Etched with Nital 2%. 100x magnification.

One important aspect that HSLA steel manufactures and the literature indicates is the homogeneity of precipitate distribution. The formation of large (>1 µm) Nb-rich precipitates particles are generally associated to interdendritic pearlitic regions, and frequently associated to MnS inclusions [17].

Figure 14 (a) and (b) demonstrate occurrences of NbC precipitated ( $\sim 1\mu\text{m}$ ) near MnS inclusions for Nb and Nb and Ti steels. For all three steels tested, sulphide inclusion were present. In long steels, after cold forming or hot/warm forging, the pieces need to be machined to obtain final shapes and tolerances. Therefore, higher sulphur content increase the challenge of long steels to achieve lower and homogeneous grain sizes.



(a)



(b)

**Figure 14.** SEM and EDS analysis of coarse NbC and MnS precipitates. (a) Al-Nb-CR and (b) Al-Nb-Ti-CR. Nital 2% etched. Magnification 3300x.

## 4 CONCLUSIONS

The main conclusions of this contribution for controlled rolling of long products are:

- It was possible to obtain significant austenitic grain refinement with Nb and Nb+Ti addition. A grain size reduction from  $30\mu\text{m}$  to  $20\mu\text{m}$  in mid radius region was obtained. However, pancaked grains in surface were heterogeneous and have showed abnormal grain growth. Characteristics of rolling process indicate that solute drag would be the main mechanism that causes recrystallization delay and grain refinement.
- Microalloying addition promoted 15% of increase in yield strength and more than 350% in absorbed energy in Charpy impact testing. Grain refinement and higher ferrite fraction should be responsible for absorbed energy increase and UTS reduction of microalloyed steels compared to Al-HR.
- Controlled rolling and microalloying addition were responsible for ferrite grain refinement, but Ti haven't enabled higher grain refinement as expected. Nevertheless, Al-Nb-Ti-CR achieved higher absorbed energy in  $-40^\circ\text{C}$ , indicating a possible lower ductile brittle transition temperature.
- Microalloyed addition and relatively low cooling rate apparently caused ferrite-pearlite banding, due to microchemical segregation of high partition coefficient (Nb and Ti).
- Coarse precipitates of NbC appeared near MnS indicating interdendritic segregation.

## Acknowledgments

The authors would like to thank Gerdau, specially Rolling Mill team and Technology of Special Steel team, and CBMM for the support in resources, time, knowledge and insights, which highly contributed for this work.

## REFERENCES

- 1 Elgert CC, Teichmann L, Bastos F, Bolota JR. Development of High Strength and High Toughness Steels. 36° Senafor. 2016; s/n.
- 2 Vervynckt S, Verbeken K, Lopez B, Jonas, JJ. Modern HSLA steels and role of non-recrystallisation temperature. International Materials Reviews. 2012; 57 (4); 187-207.
- 3 Klinkenberg C, Jansto SG. Niobium Microalloyed Steel for Long Products. New Developments in Long and Forged Products Proceedings. 2006;135-141.
- 4 Chui Z, Thermomechanical processing of structural steels with dilute niobium additions. PhD thesis. University of Sheffield. 2016; 1-235.
- 5 De Ardo AJ, Niobium in modern steels. International Materials Reviews. 2003; 48 (6); 371-402.
- 6 Rajkumar C, Increasing the yield strength of niobium microalloyed reinforcing bar. MSc thesis. University of Witwatersrand. 2008. 1-90.
- 7 Gorni AA, Steel Forming and Heat Treating Handbook. Available only online. Cited 2019, Jun 05. Available from: [http://www.gorni.eng.br/e/Gorni\\_SFHTHandbook.pdf](http://www.gorni.eng.br/e/Gorni_SFHTHandbook.pdf)
- 8 Barbosa RANM, Private communication about Nb solubility with Former-professor of UFMG and CBMM consultant. 2019, mai 27.
- 9 Gorni AA, Cálculo da temperatura de não recristalização para aços microligados, em função da interação entre a precipitação, e recristalização da austenita. Revista Escola de Minas. 1999; 52 (1); 21-25. Available from: [http://www.gorni.eng.br/Gorni\\_REM\\_Jan1999.pdf](http://www.gorni.eng.br/Gorni_REM_Jan1999.pdf)
- 10 Ouchi C, Sampei T, Kozasu I, The Effect of Hot Rolling Condition and Chemical Composition on the Onset Temperature of  $\gamma$ - $\alpha$  Transformation after Hot Rolling. Transactions ISIJ.1982; 22; 214-222.
- 11 Grozier JD, Bucher, JH. Influence du Niobium et de l'Azote sur la Résistance des Aciers a Structure Ferrite-Perlite. Revue de Métallurgie.1966; 60 (11); 939-941.
- 12 Pickering, FB. Some Aspects of the Relationships between the Mechanical Properties of Steels and their Microstructures. TISCO. Silver Jubilee Volume.1980, 105-132.
- 13 Mintz B, Peterson G, Nassar A, Structure-Property Relationships in Ferrite-Pearlite Steels. Ironmaking and Steelmaking. 1993; 21(3); 215-222.
- 14 Offerman SE., Van Dijk NH., Rekvelde, MT, Sietsma J, Van der Zwaag S. Ferrite/pearlite band formation in hot rolled medium carbon steel. Materials Science and Technology. 2002; 18;297-303.
- 15 Hashimoto S, Nakamura M, Effects of Microalloying Elements on Mechanical Properties of Reinforcing Bars. ISIJ International. 2006; 46;10; 1510-1515.
- 16 Thompson SW, Howell PR, Factors influencing ferrite/pearlite banding and origin of large pearlite nodules in a hypoeutectoid plate steel. Materials Science and Technology. 1992; 8; 777-784
- 17 Roy S, Patra S, Neogy S, Laik A, Choudary SK, Chakrabarti D, Prediction of Inhomogeneous Distribution of Microalloy Precipitates in Continuous-Cast High-Strength, Low-Alloy Steel Slab. Met. Mat. Trans. A. 2012; 43 (A); 1845-1860.